A comparison of an experimental unimolecular lifetime distribution with Rice–Ramsperger–Kassel–Marcus theory

Vincent G. Anicich, Atish D. Sen, Murray J. McEwan, and Sean C. Smith

Citation: The Journal of Chemical Physics **100**, 5696 (1994); doi: 10.1063/1.467135
View online: http://dx.doi.org/10.1063/1.467135
View Table of Contents: http://scitation.aip.org/content/aip/journal/jcp/100/8?ver=pdfcov
Published by the AIP Publishing

A comparison of an experimental unimolecular lifetime distribution with Rice–Ramsperger–Kassel–Marcus theory

Vincent G. Anicich and Atish D. Sen[a)]
Jet Propulsion Laboratory, MS 183-601, California Institute of Technology, 4800 Oak Grove Drive, Pasadena, California 91109

Murray J. McEwan[b)]
Department of Chemistry, University of Canterbury, Christchurch, New Zealand

Sean C. Smith
Department of Chemistry, University of Queensland, Brisbane, Queensland 4072, Australia

(Received 1 November 1993; accepted 7 January 1994)

The ion–molecule association system (CH_3^+/CH_3CN) has been reexamined by the ion cyclotron double resonance technique. An experimental distribution of lifetimes has been measured for the collision complex $(CH_3CNCH_3^+)^*$ formed in the association reaction between CH_3^+ and CH_3CN. The experimental mean lifetime of the association complex formed within the ICR cell was 140 μs. A theoretical examination of the distribution of complex lifetimes using an RRKM model was also undertaken. The matrix of lifetimes for the various values of the total energy of the system (E) and the total angular momentum of the system (J) was obtained. This information was used to visualize the canonical ensemble of collision complexes in the ICR experiment in terms of their lifetimes. Once the distribution of lifetimes predicted by the model was modified to conform to experimental constraints, it was found to give a good approximation of the lifetime distribution determined experimentally. As a result of the new measurements of the complex lifetimes, we report absolute values of the collisional stabilization efficiencies. We also report rate coefficients for unimolecular dissociation and radiative relaxation.

I. INTRODUCTION

Several association reactions have been studied in our laboratory[1–7] by the ion cyclotron resonance (ICR) technique. ICR is a low pressure technique in which measurements are made typically over the pressure range 10^{-7}–10^{-3} Torr. In other laboratories, higher pressure techniques such as the selected ion flow tube (SIFT) have been used to study these reactions.[8] Theoretical models to explain the experimental observations have also been developed.[9,10] Most of the laboratory studies have been concerned primarily with collisional stabilization of the intermediate $(AB^+)^*$ and the measurement of the pressure dependence of the second order rate coefficients.

One of the most important parameters of complexes formed in ion–molecule association reactions is the lifetime of the complex with respect to unimolecular dissociation. In flow tube experiments, the major stabilizing mechanism of long lived complexes is collisional stabilization. However, under conditions of interstellar clouds, 10–100 K and $<10^5$ molecule cm^{-3}, another stabilization process for the complex has been proposed as having a significant reaction rate. That process is radiative stabilization which is an important mechanism for molecular synthesis in interstellar clouds.[9] Many of the radiative association reactions proposed to occur in the interstellar medium have not been measured in the laboratory because of difficulties in detecting the complexes at sufficiently low pressures to eliminate collisions as a source of stabilization. They also often occur at rates below the detection limit of the ICR experiment. One requirement for the observation of radiative association reactions is that the lifetime of the collision complex formed in the association must be large enough to allow the radiative stabilization process of emission by ir photons to be competitive with unimolecular dissociation. Thus collision complexes having the longest lifetimes with respect to unimolecular dissociation are the most likely to have an observable radiative stabilization channel. These same complexes are also readily stabilized by collisions with a bath gas and, if the complex lives long enough to be detectable in the ICR experiment, it is usually associated with three-body collisional stabilization reaction rate coefficients that are larger than 10^{-25} cm^6 s^{-1}.

Several three-body collisional stabilization reactions have been measured that are sufficiently fast to be competitive with two-body reactions at pressures as low as 10^{-5} Torr.[2,4] This also means that some three-body reactions are likely to be significant in planetary ionospheres. Estimates of the lower limits to the mean unimolecular lifetimes of the association complexes present in fast three-body reactions have been in the range from 0.5–200 μs. These limits were established under the assumption that the third body was 100% efficient in removing energy from a collision complex. Recently we developed a double resonance ICR technique that can measure the distribution of lifetimes of long-lived collision complexes in the ICR provided unimolecular dissociation to products occurs in conjunction with stabilization.[6] Once the lifetime of the complex is known it is possible to determine explicitly the nature of the association mechanism, as absolute values for β, the stabilization efficiency, can be found. It is hoped that by understanding the association

[a)]NRC-NASA Research Associate at JPL 1989–1991.
[b)]NRC-NASA Research Associate at JPL 1986 and 1993.

 0021-9606/94/100(8)/5696/10/$6.00

mechanism in a few systems, the knowledge gained can be generalized to other systems where the complex lifetime cannot be measured.

The termolecular association reaction between an ion A^+ and a neutral B, in the presence of a buffer gas, M, is represented in Reaction (1a). The overall rate coefficient for a termolecular association, k_3,

$$A^+ + B + M \xrightarrow{k_3} AB^+ + M \tag{1a}$$

is governed largely by the unimolecular lifetime of the excited complex $(AB^+)^*$ and the rate of stabilization of the complex by the buffer gas.[1–4] The bimolecular association reaction between an ion A^+ and a neutral B is represented in Reaction (1b). The overall rate coefficient of the bimolecular reaction, k_2,

$$A^+ + B \xrightarrow{k_2} \text{products} \tag{1b}$$

depends on the lifetimes of the unimolecular processes of the complex.[2–4] The ion and the neutral are drawn together by a charge–induced dipole force for nonpolar neutrals. For polar species, an additional charge–dipole force must be considered. A collision complex, $(AB^+)^*$, is formed, as is represented in Reaction (2a)

$$A^+ + B \underset{k_{-f}}{\overset{k_f}{\rightleftharpoons}} (AB^+)^*. \tag{2a}$$

This complex is characterized by the formation rate coefficient, k_f, and the unimolecular rate for dissociation back to the reactants, k_{-f}. The complex can also dissociate into products (an ion plus a neutral) with an unimolecular rate coefficient, k_d

$$(AB^+)^* \xrightarrow{k_d} \text{products}. \tag{2b}$$

Stabilization through the emission of a photon will form an adduct ion. This radiative stabilization is represented in Reaction (2c)

$$(AB^+)^* \xrightarrow{k_r} AB^+ + h\nu. \tag{2c}$$

The radiative process is characterized by the radiative relaxation rate, k_r. A buffer gas can also relax the complex by removing the excess internal energy through collisions (collisional stabilization)

$$(AB^+)^* + M \xrightarrow{\beta k_{\text{coll}}} AB^+ + M. \tag{2d}$$

The symbol k_{coll}, is the collision rate coefficient between $(AB^+)^*$ and the buffer gas. The symbol β has traditionally been used to account for the efficiency of collisional stabilization. Values of β lie in the range $0<\beta\leqslant 1$. The bimolecular and termolecular rate coefficients which are observed experimentally are related to the rates of the elementary processes through the expressions (3a) and (3b).[2–4] We will not repeat the derivation here, but in brief k_2 is obtained by determining $d[A^+]/dt$ in the kinetic scheme defined by Eqs. (2a) through (2d) and applying a steady state approximation for $[(AB^+)^*]$. An experimental expression for $d[A^+]/dt$ is also defined from the definition for a second order rate Eq. (1b). The two expressions for $d[A^+]/dt$ are equated, yielding Eq. (3a).[2–4] The pressure derivative of the measured bimolecular rate coefficient k_2, defines the termolecular rate coefficient k_3 at the zero pressure limit. The expression defining k_3 then becomes Eq. (3b)[2]

$$k_2 = k_f(k_d + k_r)/(k_{-f} + k_d + k_r), \tag{3a}$$

$$k_3 = k_f k_{-f} \beta k_{\text{coll}}/(k_{-f} + k_d + k_r)^2. \tag{3b}$$

The mean unimolecular lifetime of the excited complex is given by the relation

$$\tau = (k_{-f} + k_d + k_r)^{-1}. \tag{4}$$

A relative stabilization efficiency can be defined for all other buffer gases with respect to stabilization by the parent gas β(B) as

$$\beta_{\text{rel}}(M) = \beta(M)/\beta(B) = k_3(M)k_{\text{coll}}(B)/k_3(B)k_{\text{coll}}(M). \tag{5}$$

The stabilization of the complex by the parent neutral B has usually been assumed in the literature[9] to occur through strong collisions.

In the association model represented by Reactions (2a)–(2d) there are five undetermined rate coefficients k_f, k_{-f}, k_d, k_r, and βk_{coll}. Four independent pieces of data are readily available:

(1) selected ion flow tube (SIFT) data which gives k_f (as long as the association is near the "pressure-saturated" regime);
(2) a low pressure ICR bimolecular rate coefficient, k_2 (which is pressure independent and determines k_d plus k_r);
(3) ICR data on the branching ratio between k_d and k_r;
(4) a higher pressure ICR result measuring the termolecular rate coefficient, k_3.

The remaining piece of experimental information needed to evaluate the five rate coefficients is a knowledge of the complex lifetime. Without a lifetime measurement an unique determination of the absolute value of the stabilization efficiency is not possible. Unfortunately in most systems, the lifetime of the complex cannot be measured directly. The double resonance method we developed for measuring the distribution of lifetimes in the ICR was first used on the collision complex formed in the reactions of HC_3N^+/HC_3N.[6] The same technique is applied here to the association complex formed from CH_3^+ and CH_3CN. The direct measurement of τ then makes it possible to determine the absolute value of β in the CH_3^+/CH_3CN system without arbitrarily assigning unit efficiency to stabilization by the parent gas as an upper limit.

We have also utilized a theoretical model of the CH_3^+/CH_3CN system from an earlier study[10] to gain further insight into the nature of the distribution of lifetimes of the complex formed in our experiments. The model uses RRKM theory with a multichannel master equation incorporating weak collisions of the complex with the bath gas. The parameters required for the RRKM treatment in our theoretical model were obtained from an *ab initio* investigation of the $C_3H_6N^+$ potential energy surface.[10] Energies of the

relevant structures were calculated at the MP4SDQ/6–311G**//HF/6–311G** level of theory. Perhaps the most sensitive of the calculated parameters to the complex lifetime, is the height of the tight transition state barrier over which the complex passes on its way to products. Some fine tuning of the calculated barrier height was made in our earlier study to achieve better agreement at low pressures with the branching ratio and pressure falloff curves found from experiment. The extent of the fine tuning was to lower the calculated *ab initio* transition state barrier height by 14%. The adjustment to the barrier height was made to achieve accord between two quite different measurements than those reported in this paper. No changes were made to any of the other *ab initio* parameters other than the usual scaling of the vibrational frequencies by 0.89. In order that we might interpret correctly the complex lifetime distribution measured by the double resonance technique, we go back to the model to extract the distribution of lifetimes of complexes formed. The model allows us to see how the lifetime distribution changes with vibrational energy and angular momenta.

In summary, we report in this paper (1) the measured distribution of unimolecular lifetimes of the complex $(CH_3CNCH_3^+)^*$ formed in the ICR by the reaction of CH_3^+ and CH_3CN. We also evaluate the values of the lifetimes, τ_{-f}, τ_d, and τ_r, and the absolute values of β, the stabilization efficiency in this system. The lifetimes are defined as the inverse of the unimolecular rates. (2) The distribution of unimolecular lifetimes of the complex $(CH_3CNCH_3^+)^*$ as predicted by the RRKM theoretical model. We then modify the theoretical distribution of lifetimes to accommodate the constraints of the ICR double resonance technique for measuring lifetime distributions.

II. EXPERIMENT

The Jet Propulsion Laboratory ICR mass spectrometer has been described in detail previously[2,7] and so only a brief description is given. The spectrometer operates in a 1.5 T magnetic field and stores ions in a trap–drift cell.[11] The ions are detected at their cyclotron frequencies by a capacitance bridge detector.[12] The drift times of the ions in the cell are measured by the method of McMahon and Beauchamp.[13] All gas pressures are measured by an ion gauge calibrated against a capacitance manometer (MKS Baratron). We have measured the temperature of the ICR cell by attaching two thin film platinum-resistance thermometers to the cell plates. One thermometer was attached to the source region trapping plate, very near to where the filament assembly is supported, and measured an equilibrium temperature of 330 K. The second thermometer was attached to the resonance region trapping plate, across the cell from the filament, and measured an equilibrium temperature of 310 K. These two temperatures represent the high and low limits of cell plate temperatures in the JPL-ICR cell. We conclude that the temperature in the JPL ICR cell is therefore 320±10 K. The bimolecular reaction rate coefficients have an estimated error of ±20% and the termolecular reaction rate coefficients have an estimated error of ±30%.

The primary ion CH_3^+ was generated by electron impact on CH_3I. The electron beam energy was maintained just above threshold for dissociative ionization of CH_3I (18 eV).

The double resonance technique to measure mean complex lifetimes developed previously[6] was used here to determine the distribution of lifetimes of the $(CH_3CNCH_3^+)^*$ collision complex. The basis of this technique is that a finite time is required to eject an ion from the ICR cell through power absorption from the double resonance oscillator. A double resonance signal is observed when a secondary ion signal is reduced by the ejection of a precursor ion. A complex ion that has a lifetime less than the ejection time will not, under normal power levels, exhibit a double resonance signal. Increasing the amplitude of the double resonance oscillator (i.e., increasing the power absorption) decreases the ejection time thereby increasing the amount of double resonance. It is the curve showing the extent of double resonance ejection against ejection time that defines the complex lifetime distribution. If the ion responsible for the double resonance has a lifetime that is greater than 1 ms, the measured apparent lifetime represents the drift time through the ICR cell at low pressure or the time between momentum transfer collisions with neutrals in the cell at higher pressures. The relationship between ion ejection time and rf amplitude is given by Eq. (6)[14]

$$t_{\text{eject}} = d^2 B / V_{rf}. \tag{6}$$

In our cell the distance from the center of the cell to the ejection plate, d, was equal to 1.27 cm, the magnetic field strength, B, was 1.5 T and the ejection voltage, V_{rf}, varied from 0 to 4.5 V_{b-p}. The required distribution of complex lifetimes is obtained from the amount of double resonance ejection at different power absorptions.

In the present case, the distribution of lifetimes of the collision complex was probed by observing the major product ion of the low pressure reaction, $C_2H_5^+$ (m/e=29).[2] Simultaneously, the adduct ion, $CH_3CNCH_3^+$ (m/e=56), was ejected from the ICR cell using various power levels. The distribution of lifetimes for $(CH_3CNCH_3^+)^*$ was then obtained from the ejection time curve.

III. RESULTS AND DISCUSSION

A. Measurement of lifetime distribution

As discussed in the Experiment section, the lifetime distribution of $(CH_3CNCH_3^+)^*$ was measured by monitoring the abundance of $C_2H_5^+$ as the association complex was ejected from the cell. Figure 1 shows the ion abundance data and a curve fitting the data that was modeled by a tenth-order polynomial. Figure 2 shows the distribution of unimolecular lifetimes of the complexes $(CH_3CNCH_3^+)^*$ that form the $C_2H_5^+$ ion. The curve in Fig. 2 was obtained by differentiating the tenth-order polynomial fit shown in Fig. 1. This distribution is similar to the behavior observed for the association complex from $HC_3N^+ + HC_3N$, $(H_2C_6N_2^+)^*$.[6] The polynomial distribution has a long tail, suggesting the existence of some very long-lived complexes. The mean unimolecular lifetime of the complex $(CH_3CNCH_3^+)^*$ from the polynomial fit was found to be τ_{av}=140 μs.

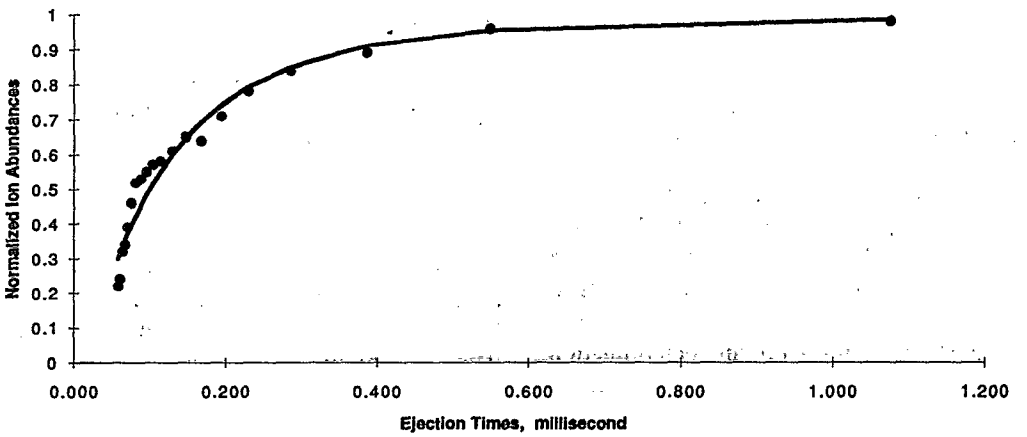

FIG. 1. Double resonance experiment. The relative signal of $C_2H_5^+$ after ejection of the precursor association ion at $m/e=56$. Different rf ejection voltages correspond to different ejection times. Here the calculated ejection times for each voltage level are plotted against the $C_2H_5^+$ signal. The dots represent the ion abundance data. The solid line represents a tenth order polynomial fit to the data.

B. CH_3^+/CH_3CN bimolecular kinetics

The reaction of CH_3^+ and CH_3CN has been studied previously by the ICR[2] (low pressure) and the SIFT[15] (high pressure) techniques. At low pressures there is a small *bimolecular association* channel with a 5% branching ratio. The overall ICR bimolecular rate coefficient was determined to be 1.8×10^{-9} cm^3 s^{-1} [2] for Reaction (7).

$$CH_3^+ + CH_3CN \rightarrow HCNH^+ + C_2H_4, \quad (7a)$$

$$\rightarrow C_2H_5^+ + HCN, \quad (7b)$$

$$\rightarrow CH_3CNCH_3^+ + h\nu. \quad (7c)$$

There is also a termolecular association channel observable at higher pressures. With CH_3CN as the third body, the termolecular rate coefficient is $k_3(CH_3CN)=1.9\times10^{-22}$ cm^6 s^{-1} and in a helium bath gas $k_3(He)=1.0\times10^{-23}$ cm^6 s^{-1} (Ref. 2)

$$CH_3^+ + CH_3CN + M \rightarrow CH_3CNCH_3^+ + M. \quad (7d)$$

At still higher pressures, as present in the SIFT experiment, the formation of collisionally stabilized adduct ions were observed and their formation rate appeared independent of pressure. A pressure-saturated rate coefficient of 4.0×10^{-9} cm^3 s^{-1} was determined for Reaction (8)[15]

$$CH_3^+ + CH_3CN + He \rightarrow CH_3CNCH_3^+ + He. \quad (8)$$

A recent re-examination of Reaction (8)[16] has revealed a slight increase in the reaction rate coefficient. An additional product ion, $HCNH^+$, was also found [Reaction (9b)]. This 12% branching ratio had been overlooked previously. We view the presence of the small $HCNH^+$ signal in the flow tube as occurring from complexes that have undergone some stabilization [represented by $(CH_3CNCH_3^+)^\sharp$] yet still have sufficient energy to cross the barrier to products as shown in Reaction (9b). The overall pseudo bimolecular SIFT rate coefficient for Reaction (9) is now 5.5×10^{-9} cm^3 s^{-1} which equals the collision rate coefficient

$$CH_3^+ + CH_3CN \rightleftharpoons (CH_3CNCH_3^+)^* \rightleftharpoons (CH_3CNCH_3^+)^* \underset{\text{collisions}}{\overset{\text{multiple}}{\rightleftharpoons\rightleftharpoons\rightleftharpoons}} CH_3CNCH_3^+ \quad (9a)$$

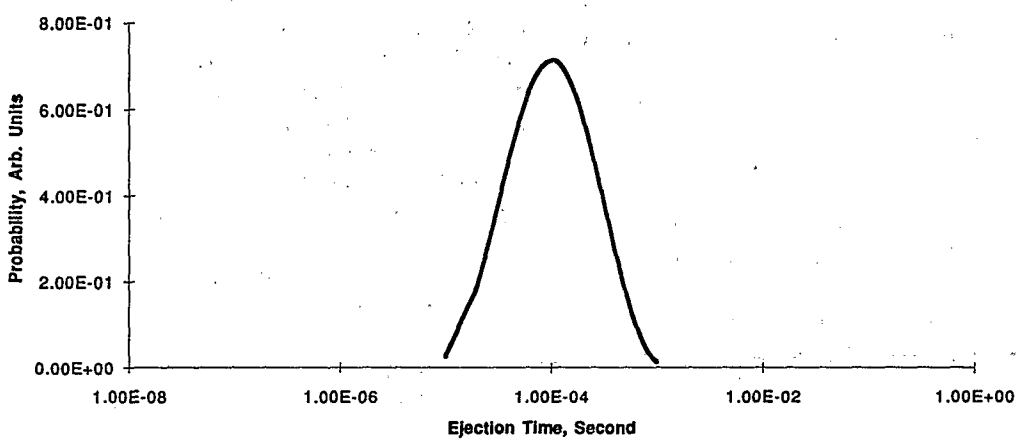

FIG. 2. Distribution of lifetimes of the collision complex $(CH_3CNCH_3^+)^*$ forming the $C_2H_5^+$ ion. The distribution shown was generated from the differentiated fit used in Fig. 1.

$$(CH_3CNCH_3^+)^{\#} \rightarrow HCNH^+ + C_2H_4. \quad (9b)$$

C. Integration of lifetime and kinetic data

SIFT measurements show that the rate coefficient for the formation of the collision complex (k_f) is equal to the collision rate coefficient. The ICR measurements on the branching ratio of product channels gives the ratio of k_d:k_r which has been measured as 0.95:0.05.[2] These data are sufficient to allow a complete analysis of the unimolecular lifetimes and rates governing the collision complex (τ_{-f}, τ_d, and τ_r). When coupled with the new complex lifetime determination of τ=140 μs, the absolute values of collisional efficiencies, $\beta(CH_3CN)$ and β(He), can be obtained. Our analysis results from the kinetic model are (1) k_f is equal to the collision rate of 5.5×10^{-9} cm^3 s^{-1}, (2) the absolute values of $\beta(CH_3CN)$ is about 0.093 and β(He) is about 0.034, (3) τ_{-f}=200 μs, τ_d=460 μs, τ_r=9.2 ms. The values of the unimolecular dissociation and radiative relaxation lifetimes are consistent with lower limits derived previously.[2] The collisional relaxation of the complex is competitive with other unimolecular processes because the unimolecular dissociation lifetime of the complex is large with a corresponding large rate coefficient for termolecular association. The radiative lifetime is typical for the emission of infrared photons for this system.[17]

A very interesting result of these studies is that collisional relaxation for removal of internal energy is inefficient which in turn means that the excess vibrational energy lost from the complex is via weak collisions *even* for the parent neutral. This conclusion is supported by the theoretical study of Smith *et al.*[10] In this study we used RRKM calculations with a master equation treatment incorporating angular momentum conservation. We were able to show that collisional relaxation of the complex by CH_3CN occurs by weak collisions for vibrational energy loss. The collisional relaxation of the complex by CH_3CN appears to occur by strong collisions for rotational energy loss. The reason for the somewhat surprising result of inefficient vibrational energy transfer when M=CH_3CN has been discussed by Smith *et al.*[10] It is a consequence of other channels competing with the association process. Our calculated values of the collisional relaxation efficiencies and the lifetime of the complex for an effective temperature of 475 K are $\beta(CH_3CN)$=0.14, β(He)=0.05, and τ=85 μs.[10] The lifetime, τ, increased to 471 μs at 300 K, and is consistent with our experimental results.

The results reported here for the efficiency of stabilization of the complex formed in the CH_3^+/CH_3CN system are consistent with results on other similar systems. RRKM calculations on the CH_3^++HCN (Ref. 18) and CH_3^++NH_3 (Ref. 19) reactions indicate that for a helium bath gas, only weak collisions could explain the pressure dependence of the rate coefficient in these systems. The assumption of a strong collision required a pressure dependent β such that the value for β necessary to fit the high pressure (SIFT) rate coefficient overestimated the rate coefficients at low pressures.

D. RRKM computer modeling

Our RRKM modeling was carried out using a FORTRAN code which has been developed in recent years for the application of microcanonical variational RRKM theory to ion–molecule, and in particular ion–dipole reactions.[10,18–20] The methodology and details of application to the CH_3^+/CH_3CN reaction have been discussed in detail in Ref. 10. In these calculations, a more accurate procedure[21] for imposing a fixed total angular momentum in the state counting for the collision complex and the tight transition state has been used.

In this work, we devote our attention to the nature of the population distribution over energy E and angular momentum J of the excited collision complex, $g^*(E,J)$. This population distribution is a crucial factor in modeling the lifetime distribution. In Ref. 10, Eq. (28), the incoming flux distribution was used for the lifetime calculations, thus

$$g^*(E,J)=g_0^*(E,J)\propto W_1(E,J)e^{-E/k_BT}, \quad (10)$$

where $W_1(E,J)$ is the sum of states evaluated variationally for the entrance (ion–dipole) channel, which is labeled as channel 1. As will be discussed more fully below, this is the population distribution of the collision complex in the short-time limit, hence the symbol $g_0^*(E,J)$.

At long times the system approaches a microcanonical steady state in the absence of collisions such that

$$g^*(E,J)=g_{ss}^*(E,J)\propto\frac{W_1(E,J)e^{-E/k_BT}}{\Sigma_i k_i(E,J)}. \quad (11)$$

The steady state distribution $g_{ss}^*(E,J)$ is clearly weighted more heavily toward lower energies and longer lifetimes than the incoming flux distribution $g_0^*(E,J)$. It is the incoming flux distribution that is used to calculate the relative lifetime probabilities shown later in the paper. In the ICR experiment, the steady state distribution is never attained and would require several seconds before it could be achieved.

Through the time-dependence of the population distribution $g^*(E,J)$, the lifetime distribution is also time dependent. We now explore the ramifications of this effect in the modeling of the time-dependent ICR experiment.

E. Theoretical lifetime distribution of $(CH_3CNCH_3^+)^*$ from RRKM model

We have accessed the RRKM model of the CH_3+/CH_3CN system reported previously[10] and retrieved the calculated flux rates for formation and loss of the complex as a function of the E,J space used in that model. The range of J values studied was from 0 to 300, and the range of energies was from 318 to 544 kJ/mol.

Figure 3 shows how the relative lifetime probabilities of all the complexes formed, change with energy and angular momenta. Each individual curve in Fig. 3 represents a specific J value but includes contributions from the different total energies, E. Each curve is also normalized separately so that all the curves will have about the same peak height for easy comparison. The lowest energies correspond to the longest lifetimes on each curve. It is apparent that there is a peaking in the distribution for each value of J. It can also be seen that the lowest values of J have the shortest lifetimes. The curves are seen to increase in lifetime from J equal to 0 up to J equal to about 160. The lifetime distributions from J

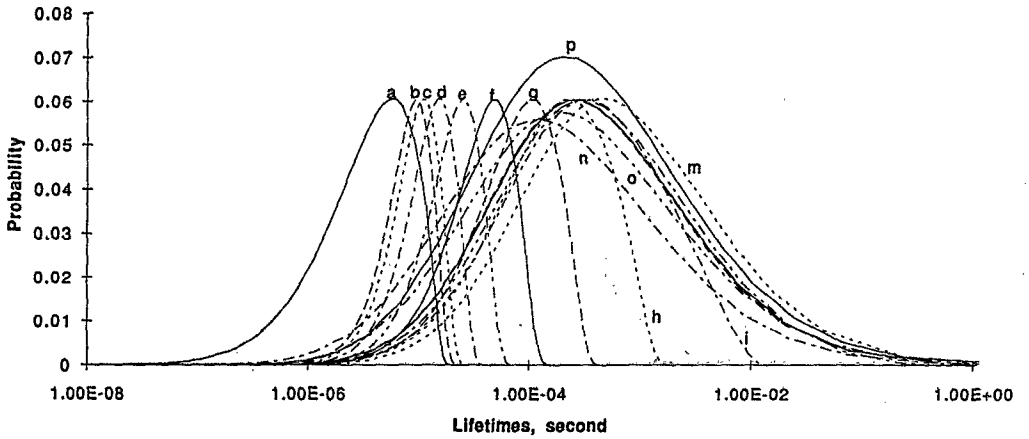

FIG. 3. The lifetime probabilities of various J levels of the collision complex $(CH_3CNCH_3^+)^*$, from RRKM theory for $T=300$ K. Each curve is for a different value of J. The J's are represented by the labels a–p, which corresponds to $J=0,20,40,...,300$. The energies sampled for each J vary between 318 and 544 kJ/mol.

equal to 160 up to J equal to 300 have approximately the same shape and distribution. The peaking of the distribution of each J curve is due to the folding in of the density of states with the Boltzmann distributions of energies. The density of states generally increases with energy, but the Boltzmann factor decreases with energy.

The trends observed in Fig. 3 may be understood by considering the contributions of the exit channel (a "tight" transition state at a barrier[10]) and the entrance channel (a "loose" transition state involving ion–dipole electrostatic interactions) to the lifetimes. Since the exit channel (denoted channel 2) is exothermic for $J=0$, $k_2(E,J)$ is already large at the threshold energy. Hence at $J=0$ the lifetimes are generally shorter with a sharp cutoff at the long lifetime/low energy side of the distribution. As the value of J increases, however, centrifugal barrier effects progressively increase the effective height of the barrier in the exit channel, thus decreasing $k_2(E,J)$ and causing the lifetimes to become longer. Ultimately, the centrifugal effect actually closes the exit channel by raising the effective barrier for the tight transition state above the reaction threshold energy. At this point one observes a qualitative change in the shape of the lifetime distribution as a broad tail towards long lifetimes develops. This tail is due to those complexes formed at low energies which cannot escape through the exit channel to products. The lifetimes of these complexes can be very long for energies close to threshold. This transition is seen to occur at around $J=160$ in Fig. 3. For higher J values the lifetime is basically controlled by the rate coefficient for dissociation back to reactants and so no major changes in the distributions occur.

Figure 4 shows the integrated population distribution of the J levels in the collision complex. The 0 and 300 J levels essentially have zero probability. The most probable value of J in the collision complex is 140. When the population factor is applied to the J curves in Fig. 3, the relative contributions of the various J levels to the total distribution of collision complex lifetimes is found and this is presented in Fig. 5. The sum of all these curves then gives a distribution of lifetimes in the collision complex and this is shown in Fig. 6.

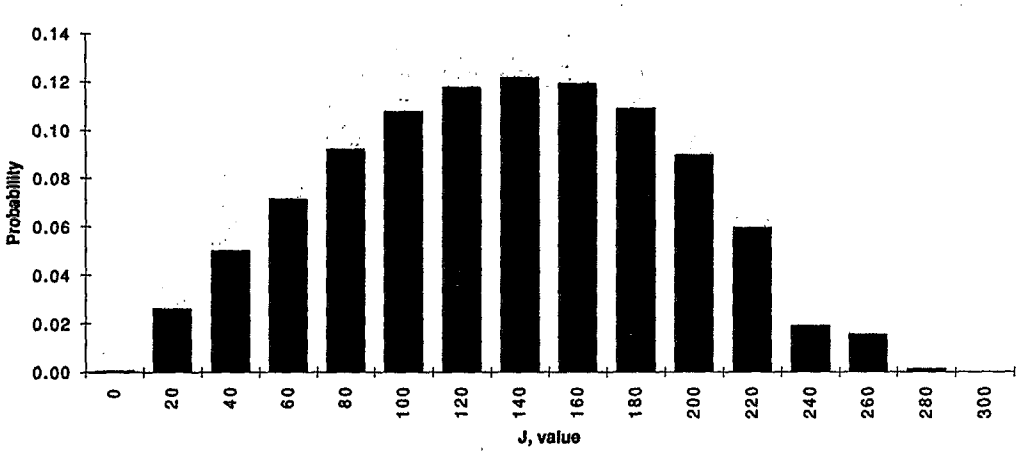

FIG. 4. The integrated population probabilities of the collision complex $(CH_3CNCH_3^+)^*$, of each J level from RRKM theory. Each bar is for a different value of J. The J's represented are $J=0,20,40,...,300$. The energies sampled for each J are from 318 and 544 kJ/mol.

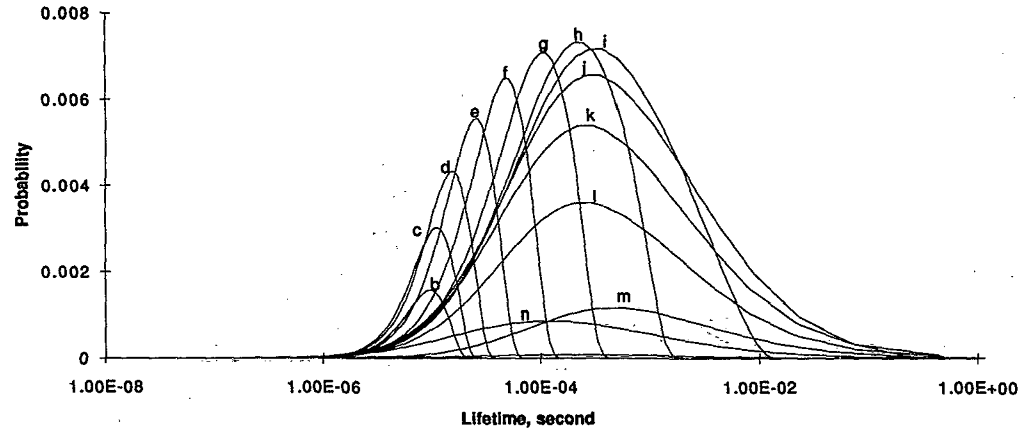

FIG. 5. The relative contributions of individual J levels of the collision complex $(CH_3CNCH_3^+)^*$, from RRKM theory and their associated lifetimes for $T=300$ K. Each curve is for a different value of J. The J's are represented by the labels a–p, which corresponds to $J=0,20,40,...,300$. The energies sampled for each J are from 318 and 544 kJ/mol.

The two curves show how the distribution of lifetimes increases as the temperature is cooled from 450 to 300 K. The reason these temperatures were chosen was that in our earlier modeling of the system,[10] the pressure falloff curves were found to give the best fit to the experimental ICR data when the effective temperature of the ions was 475 K. The distributions in Fig. 6 show the relative populations at various lifetimes for each individual collision complex formed. To understand what this means for a canonical ensemble of collision complexes, further considerations must be made.

F. Modification to theoretical lifetime distribution

It has been assumed that the distribution of lifetimes obtained from the RRKM model also represents the range of lifetimes one might expect to find from sampling the lifetimes of complexes in an ICR experiment. However, there are certain constraints within the ICR experiment that modify the modeled lifetime distributions and these need to be considered further. In the ICR drift mode operation, the electrons from the filament are modulated at 40 Hz: i.e., there is an alternating 12.5 ms ionization period followed by a 12.5 ms nonionization period. The drift time through the ICR cell is approximately 1 ms. As a reaction can occur to form a complex at any time during the 1 ms drift period, changes to the initial distribution may occur during the drift time. To cope with these modifications to the lifetime distribution within the drift period, we have modeled the formation and loss of the complex using a Runge–Kutta kinetic model. We have assumed that the average situation during the 1 ms drift period of the 12.5 ms in which the ionization is switched on, is one where reactant ions are formed initially under the electron beam. These reactant ions undergo collision with the reactant gas forming complexes. The complexes may undergo unimolecular dissociation or stabilization. The drift time in the model is divided into ten slices of time, each of 0.1 ms duration.

In the Runge–Kutta kinetic model, each collision complex formed is assigned one of 65 lifetimes. The lifetimes chosen are in the range from 10^{-7} to 2 s. The formation rate

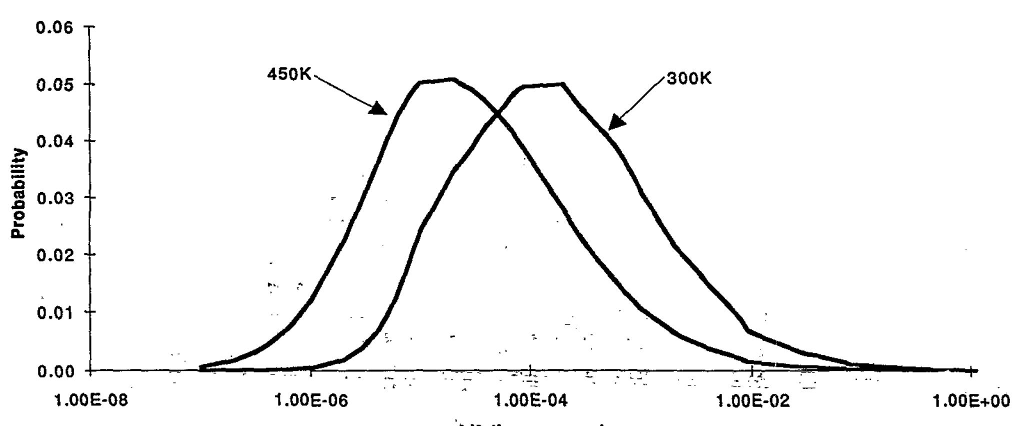

FIG. 6. The total lifetime probabilities of the collision complex, $(CH_3CNCH_3^+)^*$, from RRKM theory. Each curve is the sum over all of the various J states The two curves show the probabilities for the thermal distributions of 300 and 450 K.

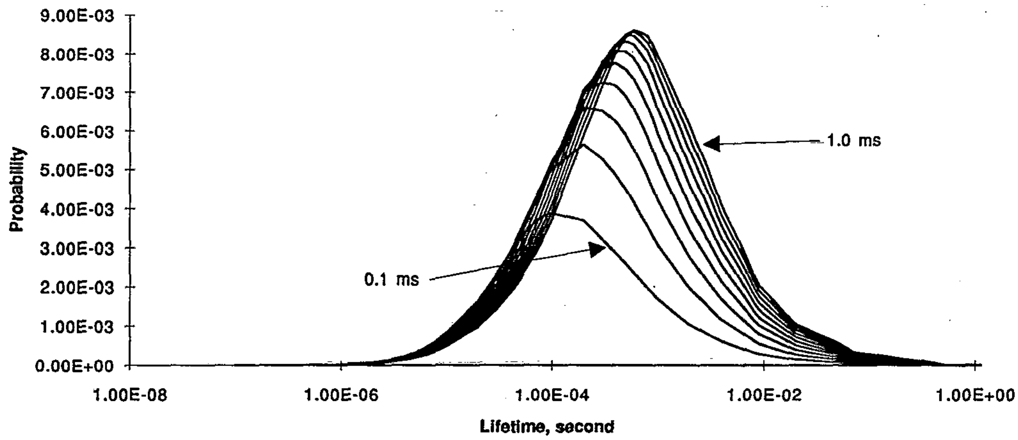

FIG. 7. The modeled distributions of lifetimes of the collision complex, $(CH_3CNCH_3^+)^*$, in the ICR cell. The figure represents the average distribution of lifetimes in a canonical ensemble of ions at 450 K, and shows the changing distribution in 0.1 ms time slices after drifting from the electron beam.

of each of the lifetime states of the collision complex was set equal to the collision rate times the probability of that lifetime being formed. The probability was taken from the RRKM averaged model at 300 K shown in Fig. 6. The evolution with time of the 65 lifetimes of the collision complex are followed during the drift time of the experiment. The collision complex was assumed to either dissociate back to reactants or products, or emit a photon to become a stable association product. The rates of dissociation were taken as the product of the inverse of the states lifetimes and the appropriate branching ratio obtained from the RRKM model. The rate of photon emission was taken as a constant of 109 per s, which is the inverse of the 9.2 ms radiative lifetime inferred from this work.

Figure 7 shows the results of the kinetic calculation. It is evident that the lifetime distribution found in the Runge–Kutta kinetics study is noticeably different from that found in the unperturbed RRKM model. Comparison with the RRKM model shows that there are substantial numbers of collision complexes that have already dissociated by the time we take our first kinetics time slice. It can also be seen that the longer the kinetics integration time, the more the longer lived species are weighted in the distribution. The peak values are found to increase from 0.1 to 1.0 ms. The eleven distributions from $t=0$ to 1 ms were summed and this total taken as the average distribution of lifetimes of all the ions in the ICR cell. The distributions calculated in the kinetic model for the temperatures 450 and 300 K are shown in Fig. 8. Thus the result of forming the complex at different times within the drift period has the effect of narrowing the distribution and weighting more heavily the longer lifetimes.

The distribution of lifetimes presented in Fig. 8 is the distribution obtained by modifying the RRKM distribution to allow for the formation of the complex at different times during the drift period and allowing the longer lived complexes to accumulate over a 1 ms period. This distribution still requires one further modification, however, before it can be used to approximate the lifetime distribution measured in the experiment and shown in Fig. 2. This final modification is a result of the constraints imposed by the double resonance

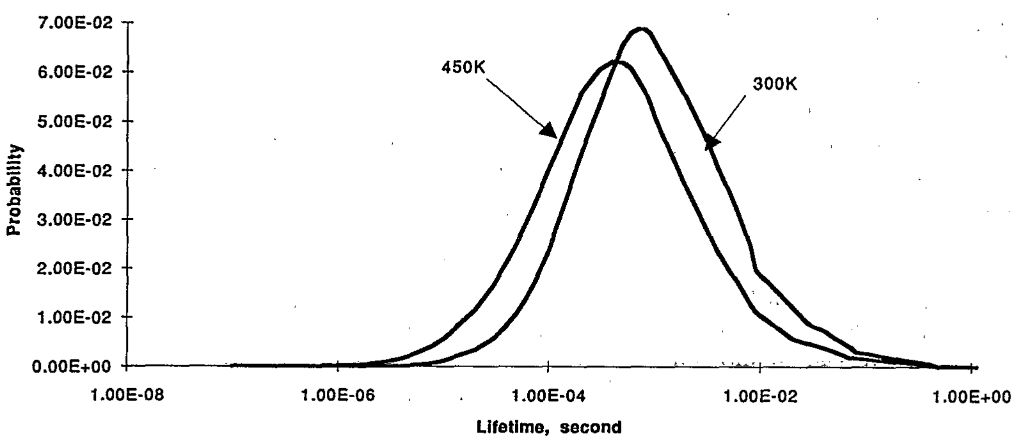

FIG. 8. The modeled distributions (which include input from the RRKM and Runge–Kutta kinetic models) of lifetimes of the collision complex, $(CH_3CNCH_3^+)^*$, in the ICR cell. These represent the average distribution of lifetimes in the canonical ensemble of ions. The curves shown represent the total of the curves in Fig. 7, for both 300 and 450 K.

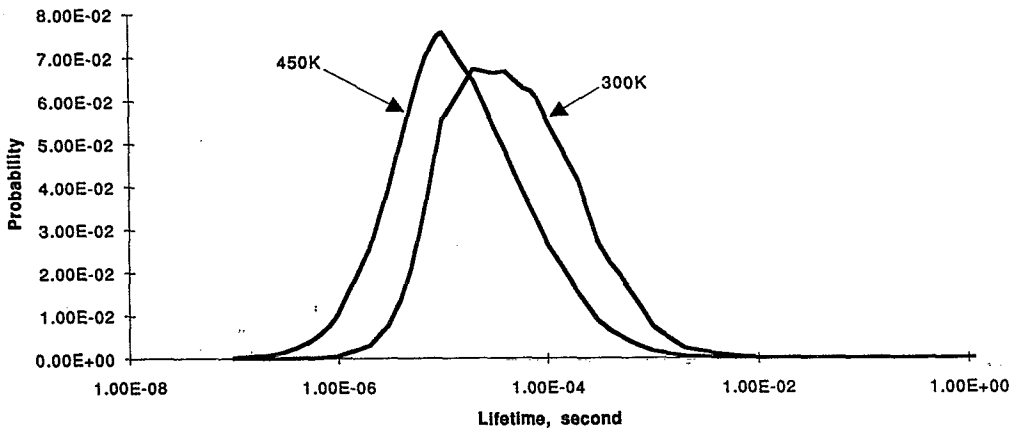

FIG. 9. The modeled distributions of lifetimes of the collision complex, $(CH_3CNCH_3^+)^*$, in the ICR cell. It differs from Fig. 8, because it represents only those collision complexes that form the dissociation product ion $C_2H_5^+$ and which are sampled during double resonance, for both 300 and 450 K.

experiment itself. As the double resonance technique samples only those complexes that undergo unimolecular dissociation to $C_2H_5^+$, it eliminates the shortest lived and the longest lived complexes from the distribution. Although in principle, very short lived complexes will be sampled in a double resonance experiment, in practice they are excluded from the experimental distribution because of a correlation between lifetime and branching ratio. The RRKM branching ratio for $C_2H_5^+$ formation (i.e., the ratio of the products to total dissociation) is not constant with energy but varies with E and J over the complex population.[10] Similarly the lifetime also varies with E and J. The branching ratio for the $(CH_3CNCH_3^+)^*$ complex toward products increases from 0.06 for those complexes with average lifetimes of 10^{-7} s, to 0.4 for those complexes with average lifetimes of 10^{-5} s. The branching ratio then decreases to zero for average lifetimes of 1 s. Thus the very shortest lived complexes are not sampled as they do not dissociate to $C_2H_5^+$ but revert instead to reactants. Similarly, the very longest lived collision complexes are not sampled by the double resonance experiment as these cannot revert to products within the drift time of the experiment.

The effect of the constraints imposed by the double resonance technique is to narrow down the distribution further. Figure 9 shows the model distribution of lifetimes with the constraints of double resonance included. This was obtained by following the formation of the $C_2H_5^+$ ion in the Runge–Kutta program, as a function of the collision complex lifetime. It is effectively the instantaneous flux distribution shown in Fig. 6 multiplied by the branching ratio of the $C_2H_5^+$ channel. The agreement between Fig. 2 (observed distribution) and Fig. 9 (calculated distribution) is reasonable bearing in mind the assumptions of the model. Part of the remaining discrepancy can be attributed to the inability of the ICR experiment to measure complex lifetimes that are less than 50 μs and part to the occurrence of nonreactive collisions which have the effect of increasing the average lifetime by lowering E, J.

IV. CONCLUSIONS

The distribution of unimolecular lifetimes of the complex $(CH_3CNCH_3^+)^*$ have been measured by the ion cyclotron double resonance technique. The mean complex lifetime under the conditions of the ICR experiment was measured as 140 μs. It is, however, obvious that many different "mean lifetimes" have been inferred in this work. Figs. 2, 6, 8, and 9 all have unique distributions of lifetimes and therefore unique mean lifetimes. Which of these are equivalent to the definition of the mean unimolecular lifetime give in the introduction as Eq. (4).

The kinetic model presented in the introduction [Eqs. (1) through (5)] is based on the observation of several measured reaction rate coefficients. The kinetic model assumes these reaction rate coefficients and branching ratios to be constant throughout the pressure ranges of the various experiments. The application of the RRKM model shows these assumptions are not valid. The calculated distribution in Fig. 6 from the RRKM theoretical model is the distribution of all complexes formed from the incoming flux distribution. It is the unperturbed distribution of complex lifetimes. The mean lifetime of this initial distribution at 300 K is 1.71 ms. Figure 8 is the average distribution of complexes modified from Fig. 6 to include reactions of the complexes through unimolecular dissociation after a drift time of 1 ms. It does include radiative stabilization. The mean lifetime of this distribution after 1 ms of processing is extended to 4.72 ms. Finally, Fig. 9 is the calculated distribution of complex lifetimes that yield $C_2H_5^+$ within the time scale of the double resonance experiment. It includes the change in branching ratios predicted by the RRKM model and the measured rate coefficients. It does not include those collision complexes with the longest and shortest lifetimes, as the RRKM model predicts these complexes do not undergo unimolecular dissociation to products at low pressure. The mean lifetime of the distribution presented in Fig. 9 (129 μs) therefore represents the best approximation from theory to the definition of lifetime pre-

sented in Eq. (4). It is also the best theoretical representation of the lifetime distribution observed in the experiment and shown in Fig. 2.

The application of RRKM modeling to the CH_3^+/CH_3CN system has aided greatly the understanding of the experimental results. We find that the complexes that contribute to the measured value of k_2, the observed bimolecular rate coefficient, come only from the center of the complex lifetime distribution. The same is not true for those complexes that undergo radiative stabilization as radiative stabilization may occur from any complex within the distribution. Clearly, however, there is a much greater probability of ir photon emission from longer lived complexes than there is from those with shorter lifetimes. The distribution from which radiative stabilization occurs has a much longer mean lifetime than the distribution shown in Fig. 9. The fact that the distribution of complexes from which k_r is measured is different from the distribution from which k_d and k_{-f} are measured does not effect the value of k_2 to any great extent as the radiative association channel amounts to only 5% of the total.

Providing appropriate knowledge of the potential energy surface is available, the RRKM model we have used provides a good description of association reactions and of the distribution of association complex lifetimes. In our earlier paper on the CH_3^+/CH_3CN system we reported how the mean lifetime varied over the temperature range 300–600 K. The low temperature limit of the model is determined by the rotational temperature of the dipole which, in the present case, will be close to 20 K. The point at which classical models tend to fail is around the rotational temperature of the dipole. Comparisons have been made between capture models (such as ours) which employ classical state counting with models using quantum adiabatic channel calculations.[22–24]

The large unimolecular lifetime exhibited by $(CH_3CNCH_3^+)^*$ is responsible for radiative relaxation channels of the complex being competitive with unimolecular dissociation channels. Collisional relaxation by the parent neutral is inefficient. This suggests that the vibrational energy loss induced by collisions is best described by a weak-collisional model as was predicted by the theoretical study.[10] The radiative decay rate of 9.2 ms for $(CH_3CNCH_3^+)^*$ implies that the radiative stabilization of the complex occurs by the emission of infrared photons.

ACKNOWLEDGMENT

The work described in this paper was carried out at the Jet Propulsion Laboratory, California Institute of Technology, under a contract with the National Aeronautics and Space Administration.

[1] M. J. McEwan, A. B. Denison, V. G. Anicich, and W. T. Huntress, Jr., Int. J. Mass Spectrom. Ion Processes **81**, 247 (1987).
[2] M. J. McEwan, A. B. Denison, W. T. Huntress, Jr., V. G. Anicich, J. Snodgrass, and M. T. Bowers, J. Phys. Chem. **93**, 4064 (1989).
[3] V. G. Anicich, A. D. Sen, W. T. Huntress, Jr., and M. J. McEwan, J. Chem. Phys. **93**, 7163 (1990).
[4] A. D. Sen, W. T. Huntress, Jr., V. G. Anicich, M. J. McEwan, and A. B. Denison, J. Chem. Phys. **94**, 5462 (1991).
[5] M. J. McEwan, V. G. Anicich, W. T. Huntress, Jr., P. R. Kemper, and M. T. Bowers, Chem. Phys. Lett. **75**, 278 (1980).
[6] V. G. Anicich, A. D. Sen, W. T. Huntress, Jr., and M. J. McEwan, J. Chem. Phys. **94**, 4189 (1991).
[7] V. G. Anicich, W. T. Huntress, Jr., and M. J. McEwan, J. Phys. Chem. **90**, 2446 (1986).
[8] D. Smith, N. G. Adams, and E. Elge, J. Chem. Phys. **77**, 1261 (1982).
[9] D. R. Bates, in *Fundamental Processes in Atomic Collision Physics*, edited by H. Kleinpoppen, J. S. Briggs, and H. O. Lutz (Plenum, New York, 1985), pp. 215–237; L. M. Bass, P. R. Kemper, V. G. Anicich, and M. T. Bowers, J. Am. Chem. Soc. **103**, 5283 (1981); J. Troe, J. Chem. Phys. **66**, 4745 (1977): **66**, 4758 (1977); E. Herbst, Astrophys. J. **313**, 867 (1987).
[10] S. C. Smith, P. F. Wilson, P. Sudkeaw, R. G. A. R. Maclagan, M. J. McEwan, V. G. Anicich, and W. T. Huntress, J. Chem. Phys. **98**, 1944 (1993).
[11] T. B. McMahon and J. L. Beauchamp, Rev. Sci. Instrum. **43**, 509 (1972).
[12] J. Wronka and D. P. Ridge, Rev. Sci. Instrum. **53**, 49 (1982).
[13] T. B. McMahon and J. L. Beauchamp, Rev. Sci. Instrum. **42**, 1632 (1971).
[14] T. A. Lehman and M. M. Bursey, *Ion Cyclotron Resonance Spectrometry* (Wiley, New York, 1976), pp. 14–18.
[15] J. S. Knight, C. G. Freeman and M. J. McEwan, J. Am. Chem. Soc. **108**, 1404 (1986).
[16] M. J. McEwan (private communication, 1992).
[17] E. Herbst and M. J. McEwan, Astron. Astrophys. **229**, 201 (1990).
[18] S. C. Smith, M. J. McEwan, and R. G. Gilbert, J. Chem. Phys. **90**, 1630 (1989).
[19] S. C. Smith, M. J. McEwan, and R. G. Gilbert, J. Chem. Phys. **90**, 4265 (1989).
[20] S. C. Smith, M. J. McEwan, and R. G. Gilbert, J. Phys. Chem. **93**, 8142 (1989).
[21] S. C. Smith, J. Phys. Chem. **97**, 7034 (1993).
[22] J. Troe, J. Chem. Phys. **87**, 2773 (1987).
[23] N. Markovic and S. Nordholm, J. Chem. Phys. **91**, 6813 (1989).
[24] S. C. Smith and J. Troe, J. Chem. Phys. **97**, 5451 (1992).